REVIEW OF TOP QUARK PHENOMENOLOGY

B. LAMPE*

Max-Planck-Institut für Physik
Werner Heisenberg Institut
P.O. Box 401212, Munich, Germany

(Received November 9, 1992)

Features of top quark physics at high energies are reviewed and developed both from a conceptual and a practical point of view, with particular emphasis on future $p\bar{p}$ and e^+e^- colliders. We study distributions and observables from which properties of the top quark can be determined. Dominant higher order corrections are taken into account and the spin structure of the various cross sections is discussed.

PACS numbers: 14.80. Dq

1. Introduction

In this article we shall discuss various aspects of top quark physics. By the top quark we mean the weak isospin partner of the b-quark. As yet there is no direct experimental evidence for the t-quark. Instead, a direct search for top quarks in high energy $p\bar{p}$ collisions at CDF has shown that $m_t > 95\text{GeV}$ [1]. Nevertheless everybody in the community seems to be convinced that it exists. In my opinion the top quark has a more definite status than the other missing ingredient of the standard model, the Higgs particle, which is a more model dependent object and relies on a paradigma about symmetry breaking.

What do we have in favour of the top? It is combination of a theoretical argument and indirect experimental evidence. It is known experimentally that the left handed b component behaves like one part of a weak $\mathrm{SU(2)_L}$ isospin doublet. For example, it has been shown that the forward backward asymmetry of the b-quark in $e^+e^- \to b\bar{b}$ which is a measure of the axial coupling of the b quark to the Z is nonzero and well compatible with the

* Heisenberg Fellow

prediction of the standard model [2]. From this we can conclude that there is a contribution of the b-quark to the axial anomaly which would render the standard model nonrenormalizable if it would not be cancelled by a corresponding t-quark contribution.

Accepting the standard model (with the t-quark) as the basis of our discussion we may look for observables where the t-quark enters through virtual effects. There are several such observables in different experiments (ARGUS [3], CLEO [3], CDF [1], CHARM [4], CDHS [4], *etc.*) For each observable one can express the prediction of the standard model as a function of m_t and, by comparing these predictions with experiment, one can check their mutual consistency and derive constraints on m_t.

This procedure will be endeavoured in Section 2. Afterwards, in Section 3, we will review top quark decay, including radiative corrections and distributions of decay products. In Section 4 top quark production in $p\bar{p}$ collision will be discussed. Of particular interest will be the inclusive production cross section $p\bar{p} \to tX$ whose prediction unfortunately is plagued by theoretical uncertainties. In Section 5 we shall elaborate on the process $e^+e^- \to t\bar{t}$ to show in how far it can be used to precisely determine top quark properties. We shall also have a look at the combined production and decay process $e^+e^- \to t\bar{t} \to \mu^+ X$ where "spin correlations" have to be taken into account.

In the whole article we shall concentrate on what we feel to be the important aspects of top quark physics. Many other features which are discussed in the literature but which we believe to be irrelevant (supersymmetric top *etc.*) are left out for the sake of clarity and stringency.

2. Precision electroweak experiments and top quark loops

The Standard Model has a sector of relatively strong coupling. This sector experimentally is difficult to access because its particles are heavy. They are the top quark and the Higgs field (both yet undiscovered) and their SU_{2L} partners, namely the left-handed b quark and the longitudinal modes of the vector bosons:

$$q_L = \begin{pmatrix} t_L \\ b_L \end{pmatrix}, t_R \quad \text{and} \quad \varphi = \begin{pmatrix} \varphi^+ \\ v + \frac{1}{\sqrt{2}}(H + i\chi) \end{pmatrix} \quad \text{where} \quad v = 174\text{GeV}$$

is the vacuum expectation value of the Higgs field. The Lagrangian for these fields reads

$$\begin{aligned} \mathcal{L}_{\text{strong}} =& \partial_\mu \varphi^+ \partial^\mu \varphi + \frac{m_H^2}{2}\varphi^+\varphi - \frac{\lambda}{4}(\varphi^+\varphi)^2 \\ &+ i\bar{q}_L \not{\partial} q_L + i\bar{t}_R \not{\partial} t_R + \Gamma_t(\bar{q}_L t_R \tilde{\varphi} + \text{h.c.}), \\ &\text{where} \quad \tilde{\varphi}^i = \varepsilon^{ij}\varphi_j^*, \end{aligned} \tag{1}$$

Γ_t and λ can be related to the top and Higgs mass, respectively, $m_t = \Gamma_t v$ and $m_H = \sqrt{\lambda} v$. Clearly, for large values m_t, $m_H = 0(v)$ the couplings Γ_t and λ are of order 1. These large couplings give in principle the dominant contributions to electroweak radiative corrections. Indeed, for observables involving light particles (*i.e.* present day energies) terms of order $\Gamma_t^2 \sim G_F m_t^2$ [$G_F = 1/2\sqrt{2}v^2$] arise in one-loop calculations, whereas terms of order λ appear only in second order.

These terms of order $G_F m_t^2$ together with the running of α account for the bulk of radiative corrections in the Standard Model. Taken together, both of these effects reproduce complicated loop calculations at the per mille level. The terms of order $G_F m_t^2$ yield the main source of information which we have at present on the value of the top quark mass. In the following we shall discuss briefly those observables from which the most stringent bounds on m_t can be deduced. We start with some quantities defined at small or zero momentum transfer and afterwards discuss information from LEP1.

A self-imposing set of input parameters for the standard electroweak theory is given by α, G_F, $m_{f \neq t}$, m_Z (known experimentally to a high level of accuracy), m_t and m_H (yet unknown). In addition, there are some other quantities (like m_W or $\sin^2 \theta_W$) which are related to the basic set of parameters. The relations are predictions of the Standard Model and should be tested in precision experiments. For example, m_W can be inferred from [5]

$$\left(1 - \frac{m_W^2}{m_Z^2}(1 - \Delta)\right) \frac{m_W^2}{m_Z^2} = \frac{\pi \alpha(m_Z)}{\sqrt{2} G_F m_Z^2}, \tag{2}$$

here $\alpha(m_Z) = 1/(128.8 \pm 0.1)$ includes the running of α which is dominated by large logarithms $\ln(m_Z/m_e)$ and

$$\Delta = \frac{3 G_F m_t^2}{8\pi^2 \sqrt{2}}, \tag{3}$$

contains the effect of electroweak radiative corrections, *i.e.* the terms of order $G_F m_t^2$ as discussed above.

Now a comparison to the measured value m_W/m_Z from $p\bar{p}$ collisions at CDF can be made and a range for m_t can be deduced, $m_t = 150 \pm 50$GeV.

$\sin^2 \theta_W$ can be defined in a number of ways [6]. We prefer the definition where the ratio between electromagnetic and weak neutral and charged currents is given in terms of $\sin^2 \theta_W$ and unchanged by higher order effects,

$$\begin{aligned} \mathcal{I}_{em}^f &\sim \gamma_\mu Q_f, \\ \mathcal{I}_Z^f &\sim \gamma_\mu \left[I_3^f (1 - \gamma_5) - 2 Q_f \sin^2 \theta_W \right], \\ \mathcal{I}_W^f &\sim \gamma_\mu (1 - \gamma_5), \end{aligned} \tag{4}$$

(for fermions $f \neq b$. The case $f = b$ will be discussed later.) This ratio, and therefore $\sin^2\theta_W$, have been obtained by the CHARM and CDHS collaborations at CERN [7]. The so called ρ parameter is defined as the deviation of this ratio from the ratio of masses, m_W/m_Z, more precisely

$$\sin^2\theta_W = 1 - \frac{m_W^2}{\rho m_Z^2}, \tag{5}$$

ρ can be calculated in the Standard Model from the diagrams in Fig. 1. It turns out that

$$\rho_{SM} = 1 + \Delta. \tag{6}$$

This can be compared to the experimental result ρ_{exp} and a range for m_t can again be deducted, $m_t = 120 \pm 50\text{GeV}$.

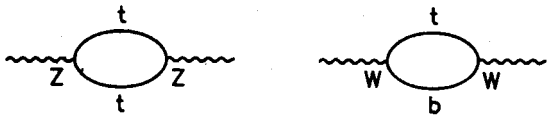

Fig. 1.

Terms of order $G_F m_t^2$ are also contained in observables measured to a high precision by the LEP experiment [6–9]. Quantities like the width Γ_l for Z going into charged leptons and the corresponding forward backward asymmetries can be used to infer constraints on the value of m_t. The lowest order expressions

$$\Gamma_l = \frac{\alpha}{3} m_Z a_l^2 \left(1 + \left(\frac{v_l}{a_l}\right)^2\right) \tag{7}$$

and

$$A_{FB}^l = 3 \left(\frac{\frac{v_l}{a_l}}{\left(\frac{v_l}{a_l}\right)^2 + 1} \right)^2, \tag{8}$$

where $a_l = I_3^l/2\sqrt{y}$, $(v_l/a_l) = 1-(Q_l/I_3^l)(1-\sqrt{1-4y})$, $y = (\pi\alpha/\sqrt{2}G_F m_Z^2)$ and $I_3^l = -1/2$ show that Γ_l and A_{FB}^l are measures of the vector and axial vector couplings v_l and a_l of the Z to the leptons. Note that y is defined in terms of the fundamental quantities α, G_F and m_Z. The asymmetry in (8) is defined to be obtained from the data after deconvolution of initial state radiation because it would otherwise be dominated by large logarithms $(\alpha/\pi \ln(m_Z/m_e))^n$. Deviations from the lowest order expressions can be

parameterized [9, 10] by introducing effective couplings

$$a_l \to a_l \left(1 + \frac{\Delta}{2}\right) = a_l^{\text{eff}},$$
$$\frac{v_l}{a_l} \to \frac{v_l}{a_l} + 2\frac{Q_l}{I_3^l}\frac{y}{\sqrt{1-4y}}\Delta = \left(\frac{v_l}{a_l}\right)_{\text{eff}}, \tag{9}$$

with $\Delta = (3G_F m_t^2/8\sqrt{2}\pi^2)$ defined earlier. Of course, this special parameterization a_l^{eff} and v_l^{eff} is reasonable only for the specific observables under consideration, Γ_l and A_{FB}^l. In Figs 2 and 3 the predictions for Γ_l and A_{FB}^l are drawn as a function of m_t and compared with the latest LEP results. These figures lead us to conclude that $m_t = 100 \pm 60\text{GeV}$ (from Γ_l) and $m_t = 170 \pm 60\text{GeV}$ (from A_{FB}^l).

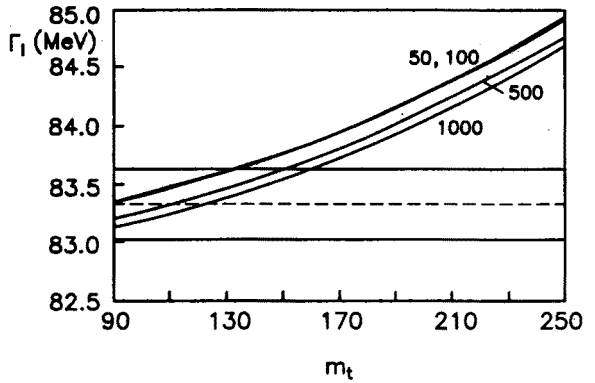

Fig. 2.

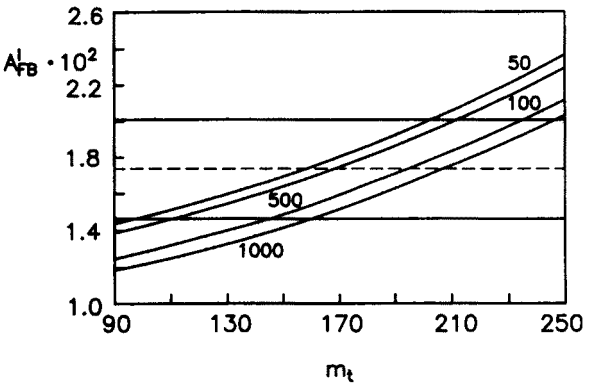

Fig. 3.

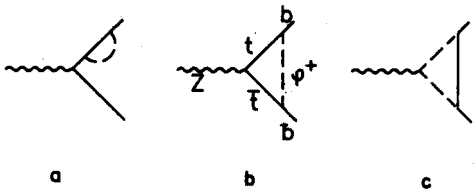

Fig. 4.

The leptonic quantities Γ_l and A_{FB}^l are very likely to follow the Standard Model predictions. Therefore I judge the efforts made in the literature to rewrite deviations from the tree level relations(7,8) in terms of SM independent quantities S,T,U [11] or $\varepsilon_1,\varepsilon_2,\varepsilon_3$ [7, 12] superfluous. A different thing might be the corresponding quantities Γ_b and A_{FB}^b for the bottom quark. In my opinion they are of particular importance because of large m_t terms in the $Zb\bar{b}$ vertex. As a final application of the terms $G_F m_t^2$ let us have a look at these quantities. The main difference as compared to lepton production comes from the diagrams in Fig. 4 because they involve the top quark and its Yukawa coupling. Due to SU_{2L} symmetry they give a correction $\sim 1-\gamma_5$ to the lowest order $Zb\bar{b}$ vertex [13]. We write

$$\Gamma_\mu^{Zb\bar{b}} = ie\gamma_\mu(v_b - a_b\gamma_5) + ie\gamma_\mu F(1-\gamma_5)\,, \tag{10}$$

where $a_b = (I_3^b/2\sqrt{y})$, $(v_b/a_b) = 1-(Q^b/I_3^b)(1-\sqrt{1-4y})$, $Q_b = -1/3$, $I_3^b = -1/2$ and y was defined after Eq. (8). $F = F_{SM} = F_a^{SM}+F_b^{SM}+F_c^{SM}$ is the contribution from the diagrams Fig. 4(a),(b),(c). A simple calculation gives

$$\begin{aligned}
F_a^{SM} &= -\frac{3e^2}{16\pi^2}\,\frac{v_b+a_b}{16s_W^2}\,\frac{m_t^2}{m_W^2}\,,\\
F_b^{SM} &= +\frac{e^2}{16\pi^2 4s_W^2}\,\frac{m_t^2}{m_W^2}\left(\tfrac{3}{4}v_t+\tfrac{5}{4}a_t\right)\,,\\
F_a^{SM} &= +\frac{3e^2}{16\pi^2}\,\frac{m_t^2}{m_W^2}\,\frac{s_W^2-c_W^2}{32s_W^3c_W}\,.
\end{aligned} \tag{11}$$

Therefore

$$F_{SM} = \frac{1}{16\pi^2}\,\frac{G_F m_t^2}{\sqrt{2}s_W c_W} = -\frac{2}{3}a_b\Delta \tag{12}$$

which can be interpreted as an (identical) change in the Born couplings v_b and a_b of the order of 1%. This change is to be added to the changes (9) which a_b and v_b experience in the same way as a_l and v_l. Note that within the terms of order $G_F m_t^2$ any definition of $\sin^2\theta_W$ is convenient.

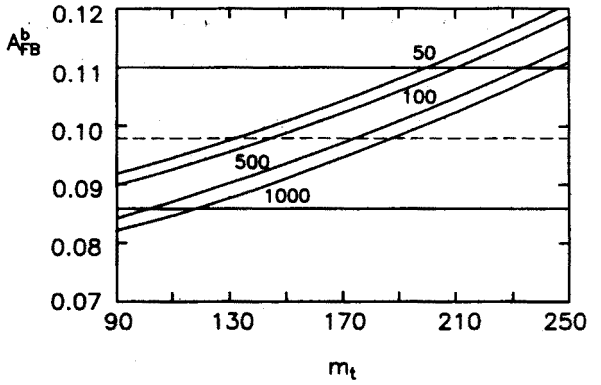

Fig. 5.

Terms of the form $\sigma_{\mu\nu}Z^\nu$ and b_μ *etc.* need not be considered because they lead to contributions to Γ_b and A_{FB}^b which are suppressed by powers of m_b/m_Z.

Before a comparison with experimental data can be made several issues have to be settled. First, since we are dealing with quarks we have to take QCD corrections to A_{FB}^b and Γ_b into account. These are now known to second order α_s^2 [14, 15] and can be pulled out of the experimental numbers to define "electroweak" quantities $(\Gamma_b)_{\rm ew}$ and $(A_{FB}^b)_{\rm ew}$. Secondly, for A_{FB}^b, $B^o - \overline{B}^o$ mixing has to be taken into account, *i.e.* there is a certain probability that a b-quark escapes detection in one hemisphere because it transforms into an anti b (and vice versa). This can be corrected for, and in the following we assume to talk about the corrected forward backward asymmetry.

The prediction for these quantities is

$$(\Gamma_b)_{\rm ew} = N_c \frac{\alpha}{3} m_Z a_{b\,\rm eff}^2 \left[1 + \left(\frac{v_b}{a_b}\right)^2_{\rm eff}\right], \tag{13}$$

$$\left(A_{FB}^b\right)_{\rm ew} = 3 \frac{\left(\frac{v_e}{a_e}\right)_{\rm eff}}{1 + \left(\frac{v_e}{a_e}\right)^2_{\rm eff}} \frac{\left(\frac{v_b}{a_b}\right)_{\rm eff}}{1 + \left(\frac{v_b}{a_b}\right)^2_{\rm eff}}, \tag{14}$$

with $a_e^{\rm eff}$ and $(v_e/a_e)_{\rm eff}$ as in (9) and

$$a_b^{\rm eff} = a_b \left(1 - \tfrac{2}{3}\Delta\right)\left(1 + \tfrac{1}{2}\Delta\right), \tag{15}$$

$$\left(\frac{v_b}{a_b}\right)_{\rm eff} = \frac{\frac{v_b}{a_b} + 2\frac{Q_b}{I_3^b}\frac{y}{\sqrt{1-4y}}\Delta - \frac{2}{3}\Delta}{1 - \frac{2}{3}\Delta}, \tag{16}$$

where $(v_b/a_b) = {}^1\!/_3(1 + 2\sqrt{1-4y})$.

In Fig. 5 we compare the prediction for $(A_{FB}^b)_{ew}$ with the latest experimental results. This comparison yields a top quark mass range $m_t = 160 \pm 80\text{GeV}$. The experimental uncertainty is quite large due to ambiguities associated with semileptonic branching ratios (b quark mixing and charm decays) and, in my opinion, the present experimental result should be considered with some scepticism.

Since the b quark is the heaviest quark so far detected, it is conceivable that nonstandard effects are discovered first in connection with Γ_b or A_{FB}^b, more specifically, that they arise through deviations from the Standard Model diagrams Fig. 4. I think it is really an interesting possibility that new interactions between the heavy particles of the Standard Model exist, *i.e.* between Higgs field and the top quark, and, through SU_{2L} symmetry, between the Higgs doublet and the quark doublet (t_L, b_L) so that in particular the $tb\varphi^+$ vertex which is of order Γ_t and appears repeatedly in Fig. 4 is modified. This possibility can be studied systematically in the framework of an effective Lagrangian approach by adding $SU_{2L} \times U_1$ symmetric dimension six interactions to the Standard Model Lagrangian (1) [16]. It leads to changes in the quantity F which are of the same order of magnitude as the Standard Model contribution F_{SM} (12) (changes at the per cent level). As soon as the LEP1 data have reached this level of accuracy we can therefore hope to get insight in possible new interactions within the heavy sector of the Standard Model. I believe that precise measurements of b properties at LEP1 is a very useful device for looking beyond the Standard Model at a time where the discovery of the top quarks is still ahead of us.

On the basis of the present experimental knowledge, I conclude that the top quark should be in the range between 120 and 200 GeV. If there is physics beyond the Standard Model this expectation has to be revised. For example, the upper bound is very strongly influenced by the experimental constraints from the ρ-parameter ($\rho_{exp} = 1.007^{+0.005}_{-0.003}, \rho_{SM} = 1 + (3G_F m_t^2/8\sqrt{2}\pi^2)$). For extensions of the Standard Model with new contributions to the ρ-parameter the upper value of 200 GeV should be shifted accordingly.

A priori, and from its construction, the top quark is entirely a Standard Model object. Nevertheless, it may prove to be an ideal place to look for nonstandard physics, because it is the matter field with the largest mass. Therefore, from time to time in the course of this work, we shall have a quick look on possible signatures of new physics. The combination of Standard Model physics still to be checked and the exciting possibility of something unexpected makes top quark phenomenology so interesting.

In the mass range 120–200 GeV the top quark decays before resonance formation and hadronization because its width is much larger than Λ_{QCD}. We will often recur to perturbative considerations in the course of this work.

Let us now have a closer look at the top quark width.

3. Top quark decay

3.1. Total rate

The dominant decay mode for top quarks in the Standard Model is $t \to bW^+$. To a high degree of accuracy (<1%) the width of the top quark is predicted to be

$$\Gamma(t \to bW^+) = \frac{G_F m_t^3}{8\sqrt{2}\pi}\left(1 - \frac{m_W^2}{m_t^2}\right)^2\left(1 + 2\frac{m_W^2}{m_t^2}\right)\left(1 - C_F\frac{\alpha_s}{2\pi}f\right)(1 + \delta_{ew}), \tag{17}$$

where the QCD correction is given by

$$f = \frac{2}{3}\pi^2 - \frac{5}{2} + O\left(\frac{m_W^2}{m_t^2}\right), \quad (\text{for} \quad m_t \gg m_W) \tag{18}$$

and δ_{ew} stand for the electroweak correction term whose leading contribution of order $G_F m_t^2$ is given by the Higgs exchange diagram (Fig. 6).

$$\delta_{ew} = \frac{G_F m_t^2}{4\sqrt{2}\pi^2}\left(\frac{17}{4} + \ln\frac{m_H^2}{m_t^2}\right) + \text{subleading terms} \tag{19}$$

which is 0.02 for $m_H = O(m_t)$ and the subleading terms are such that $\delta_{ew} \approx 0.02$ remains true even for $m_H \neq O(m_t)$ [17]. In these results terms of order $m_b^2/m_t{}^2$ as well as corrections due to CKM mixing have been neglected.

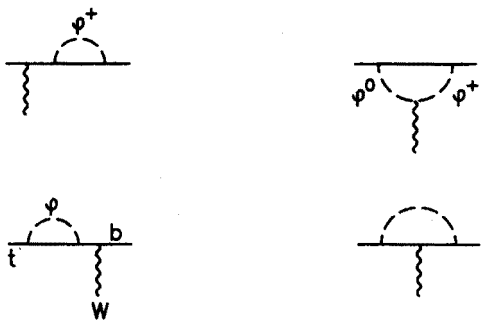

Fig. 6.

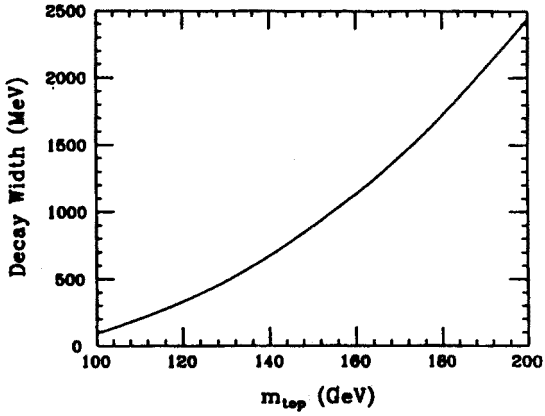

Fig. 7.

The W^+ will consequently decay into one of the three lepton doublets or one of the $2N_c$ light quark doublets. As a consequence a factor $[3 + 2N_c(1 + {}^3/_2\, C_F\, \alpha_s/2\pi)]^{-1}$ appears in branching fractions for leptonic W decays.

In Fig. 7 $\Gamma(t \to bW^+)$ is drawn as a function of m_t including higher order corrections. $\Gamma(\sim {m_t}^3)$ increases rapidly with m_t and in the region $\Gamma \gg \Lambda_{\mathrm{QCD}}$ (corresponding to $m_t > 120$ GeV — the mass region considered in this article) a top quark will generally decay before hadronization occurs. This permits top quark phenomenology to be treated pertubatively, allowing a more accurate analysis than is possible for longer lived quarks.

3.2. Muon energy spectrum

The most interesting decay channel in the sense of cleanest experimental signature is $t \to \mu^+ \nu_\mu b$. Due to the real W intermediate state this process is in many respects much different than the corresponding process $b \to \mu^- \nu_\mu c$. For example, one may study the distribution in the muon energy $E_l = (m_t/2)\, x_l$ for a top quark at rest. The result is

$$\frac{d\Gamma}{dx_l} = \frac{3G_F {m_t}^3}{4\sqrt{2}\pi}\left[x_l(1 - x_l) - C_F \frac{\alpha_s}{2\pi} F_1\left(x_l, \frac{{m_W}^2}{{m_t}^2}\right)\right], \tag{20}$$

where, for kinematical reasons, $x_l \in [{m_W}^2/{m_t}^2, 1]$ and the QCD correction factor F_1 was calculated in the comprehensive study by Jeżabek and Kühn

[18]. It turns out to be moderate (<100%) except for the end point of the spectrum where it is well known that an all orders summation of gluon effects has to be done [19].

The muon energy is the central variable for the process $t \to \mu^+ \nu_\mu b$ (in the cms of the top quark). All other kinematical quantities are either trivial or can be deducted from it.

3.3. Spin terms

Since nonperturbative effects are small for the top system spin correlations are not washed out for a process in which a t quark is produced with a polarization vector s and subsequently decays. The decay $t \to \mu^+ \nu_\mu b$ has a very simple matrix element,

$$\begin{aligned} |M|^2 &\sim \mathrm{tr} \not{b} \gamma_\alpha P_- (\not{t} + m_t) \tfrac{1}{2}(1 + \gamma_5 \not{s}) \gamma_\beta P_- \mathrm{tr} \not{\nu} \gamma_\alpha P - \not{\mu} \gamma_\beta P_- \\ &\sim [(t - m_t s)\mu][b\nu] \,. \end{aligned} \tag{21}$$

This leads to an angular distribution of the form

$$\frac{d\Gamma}{dx_l d\cos\theta} = \frac{d\Gamma}{dx_l} \frac{1}{2}(1 + \cos\theta) \,, \tag{22}$$

where $\theta = \sphericalangle (\vec{s}, \vec{W})$ and $d\Gamma/dx_l$ was given in (20). The factorization is a consequence of the $V - A$ interaction between t,W and b, and, apart from tiny deviations, remains true if one includes the higher order corrections [20]. It would be violated, however, by nonstandard interactions, like $V + A$ *etc.*

4. Top quark production in $p\bar{p}$ collisions

The top quark will be discovered by the process $gg \to t\bar{t}$ in high energy $p\bar{p}$ collisions, *cf.* Fig. 8.

Fig. 8.

Due to the softness of the gluon distribution inside the proton most of the top quarks will come from soft gluons $x_{1,2} \ll 1$ and will be produced nearly at rest, $s = x_1 x_2 S \simeq 4m_t{}^2$.

The parton level cross section $\sigma(gg \to t\bar{t})$ (which is of order α_s^2) is well known and one-loop QCD corrections of order α_s^3 to it have been calculated

[21]. Among these the dominant contribution comes from the diagram in Fig. 9 where there is first an order α_s^2 gluon gluon scattering process followed by a gluon splitting into a $t\bar{t}$ pair. This contribution can become of the same order of magnitude as the leading order contribution because the cross section for $gg \to gg$ is large as compared to the cross section for gg $\to$ quarks. One may hope, with some justification, that the two-loop effects are moderate so that the theoretical error inherent in the one-loop result is under control provided a reasonable choice of scale (argument of α_s) is made which I suggest to be the transverse momentum p_T for the p_T distribution and $2m_t$ for the integrated cross section.

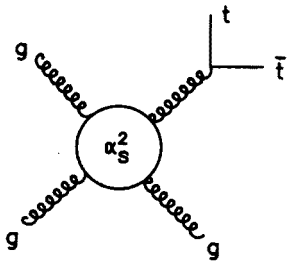

Fig. 9.

Near threshold cross sections are known to be affected by resonance effects. However, due to averaging over gluon x these effects are less spectacular than in e^+e^- annihilation. This will be discussed in detail in Section 5. Electroweak effects (*e.g.* from virtual exchange of the Higgs particle) have also proven to be small.

In fact, I think that the most important source of uncertainty is not of theoretical origin, is not (perturbative) QCD, but is a phenomenological one: it stems from our missing knowledge of the precise form of the gluon distribution at small x. One can show that the prediction for the cross section $\sigma(p\bar{p} \to tX)$ varies by almost 30% according to which parametrization of the gluon structure function is chosen. The problem with the gluon distribution is that there is no clean process which allows its accurate determination. In ep collisions from which the gluon density is usually deducted the gluon process $g\gamma^* \to$ anything contributes only in higher order α_s (compared to the leading order process $q\gamma^* \to$ anything). In effect, results for the cross section $\sigma(p\bar{p} \to tX)$ as presented in the literature are not much better than estimates, and the more so the higher the energies are. Going from 1.8 (Tevatron) to 16 TeV (LHC) one gains about two orders of magnitude in rate, but also two orders of magnitude in uncertainty because at 16 TeV the gluon distribution is probed at smaller values of x. In spite of these deficiencies in Table I we show estimates for the total cross section

for top quark production for several values of m_t and s. Let me repeat that the bulk of this cross section arises at small p_T

TABLE I

Integrated top quark production cross section in pb including the theoretical error from perturbative QCD and the phenomenological error from ignorance about the gluon structure functions. To estimate this error several parametrizations of structure functions have been used [22].

m_t	$\sqrt{s} = 1.8$ TeV	$\sqrt{s} = 16$ TeV
100	90.0 ± 30.0	11000 ± 2000
120	34.0 ± 11.0	4300 ± 1000
140	15.0 ± 4.0	2200 ± 500
160	7.0 ± 2.0	1200 ± 300
180	3.8 ± 1.0	750 ± 150
200	1.9 ± 0.5	450 ± 100

At the end of this section let me make a short remark about spinterms. These are needed in $e^+e^- \to t\bar{t}$ if one wants to combine the prediction of a top quark with its subsequent decay and will be discussed in detail in the next section. However, it can easily be seen that the spinterms do not contribute in case of the process $gg \to tX \to bW^+X$. The reason is that the coupling between top quark and gluon is purely vectorlike with no axial admixture.

5. Top quark production in e^+e^- annihilation, and its subsequent decay

In the last sections we have seen that $p\bar{p}$ collisions are a helpful tool to produce and discover the top quark and, by studying its decay, to fix its properties like mass and couplings to an accuracy of order 5–10% (for mass) and 20–50% (for couplings). To make more precise measurements, however, an e^+e^- machine operating at our above $t\bar{t}$ threshold is the appropriate device [23].

In principle there is a variety of reactions that gives us top quarks at an e^+e^- collider. However, at energies accessible in the foreseeable future (< 1 TeV) all reactions except e^+e^- annihilation into γ and Z (Fig. 10) completely negligible.

The cross section can be expanded in powers of the cosine of the production angle θ, with coefficients called σ_U, σ_L and σ_P.

$$\frac{d\sigma}{d\cos\theta} = \tfrac{3}{8}(1+\cos^2\theta)\sigma_U + \tfrac{3}{4}\sin^2\theta\sigma_L + \tfrac{3}{4}\cos\theta\sigma_P\,, \qquad (23)$$

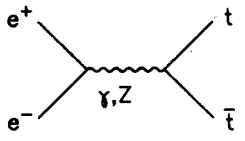

Fig. 10.

U and L denote the contributions of unpolarized and longitudinally polarized γ and axial vector coupling. In the integrated cross section $\sigma = \sigma_U + \sigma_L$, σ_P drops out. It is, however, measured by means of the forward backward asymmetry

$$A_{FB}^b = \left(\left[\int_{-1}^{0} - \int_{0}^{1}\right] d\cos\theta \frac{d\sigma}{d\cos\theta}\right)\left(\left[\int_{-1}^{0} + \int_{0}^{1}\right] d\cos\theta \frac{d\sigma}{d\cos\theta}\right)^{-1}$$
$$= \frac{3}{4}\frac{\sigma_P}{\sigma_U + \sigma_L} \tag{24}$$

Explicit expressions for σ_U, σ_L and σ_P are known in lowest order:

$$\sigma_U = [\beta\sigma_{VV} + \beta^3\sigma_{AA}]\pi\alpha^2 ,$$
$$\sigma_L = \frac{2m_t^2}{s}\beta\sigma_{VV}\pi\alpha^2 ,$$
$$\sigma_P = \beta^2\sigma_{VA}\pi\alpha^2 \tag{25}$$

with

$$\sigma_{VV} = 4\frac{Q_e^2 Q_t^2}{s} + 8Q_e Q_t v_e v_t \frac{s - m_Z^2}{D} + 4\left(v_e^2 + a_e^2\right)v_t^2 \frac{s}{D} ,$$
$$\sigma_{AA} = 4\left(v_e^2 + a_e^2\right)a_t^2 \frac{s}{D} ,$$
$$\sigma_{AV} = 8Q_e a_e Q_t a_t \frac{s - m_Z^2}{D} + 16 v_e a_e v_t a_t \frac{s}{D} \tag{26}$$

and $D = (s - m_Z^2)^2 + (s^2\Gamma_Z^2/m_Z^2)$.
The fermion couplings are given by

$$v_f = \frac{I_3^f - 2Q_f s_W^2}{2 s_W c_W} , \quad a_f = \frac{I_3^f}{2 s_W c_W} . \tag{27}$$

One can work out the numerical details and, for $m_t = 0(150\text{GeV})$, finds the cross section to be of order $R = \sigma(e^+e^- \xrightarrow{\gamma} \mu^+\mu^-) = 4\pi\alpha^2/3s$ becoming somewhat larger than R far above threshold [24]. In all these considerations it is assumed that the top quarks are on shell.

The dominant radiative corrections are the following:

- large electroweak radiative corrections of the $G_F {m_t}^2$ due to Higgs exchange. They can be incorporated in a redefinition of the charge factors in (26) and are somewhat larger (0(5%) in the threshold region for $m_H \geq 0(m_t) = 150\text{GeV}$) than in the case $Z \to b\bar{b}$ (1%). They are really important only for rather light Higgs bosons ($m_H \ll m_t$) [25].
- large electroweak corrections of the form $\alpha \ln(s/m_e^2)$. They can be incorporated by introducing a running $\alpha(s)$ in (25) and a deconvolution of initial state radiation.
- QCD enhancement factors can be parametrized by [15, 26]

$$\sigma_{VV} \to \sigma_{VV}\left[1 + C_F\alpha_s\left(\frac{\pi}{2\beta} - \frac{3+\beta}{4}\left(\frac{\pi}{2} - \frac{3}{4\pi}\right)\right)\right],$$
$$\sigma_{AA} \to \sigma_{AA}\left[1 + C_F\alpha_s\left(\frac{\pi}{2\beta} - \left(\tfrac{19}{10} - \tfrac{22}{5}\beta + \tfrac{7}{2}\beta^2\right)\left(\frac{\pi}{2} - \frac{3}{4\pi}\right)\right)\right] \quad (28)$$

where in my opinion the argument of α_s should be chosen to be s.

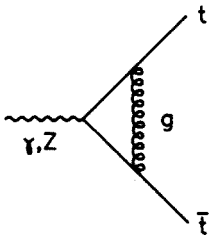

Fig. 11.

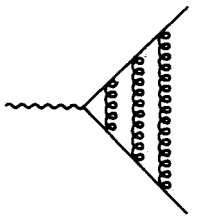

Fig. 12.

Far enough above threshold these QCD enhancement factors are typically of the order of +10% and somewhat larger than the electroweak corrections which are negative. At very high energies they converge to the familiar factor $1 + \alpha_s/\pi$ of the massless theory whereas near threshold they are dominated by the term $\sim 1/\beta$. This terms although compensated by the phase space $\sim \beta$ is a signal of the Coulomb singularity which arises in higher order for $\beta \to 0$ (threshold). In order α_s it is induced by the virtual correction Fig. 11 and in higher orders by ladder diagrams like in Fig. 12. For top quarks at rest these contributions can be summed so that the Coulomb singularity is regulated and a finite cross section for $\beta = 0$ emerges [24, 27]. It is interesting to describe the dependence of the $t\bar{t}$ production cross section on m_t. For large values $m_t > 180\text{GeV}$ no remnant of resonance formation can be seen in the integrated cross section $\sigma_{\text{tot}}(s)$ as a function of energy $E = \sqrt{s}$ (*cf.* Fig. 13). For $m_t \in [120, 180]\text{GeV}$ there is one peak in $\sigma_{\text{tot}}(s)$ near threshold which rapidly decreases for $m_t \to 180\text{GeV}$ and which is a remnant of many overlapping Breit Wigner resonances (their width being much larger than their energy separation). Since it is technically difficult to sum the contributions from a large number of radial excitations one should directly calculate the imaginary part of Green's function for complex energy [24, 27, 28]. Namely, at threshold, we have

$$\sigma(e^+e^- \to t\bar{t}) = \frac{24\pi^2\alpha^2}{s{m_t}^2}\left(1 - 8C_F\frac{\alpha_s}{2\pi}\right)\rho_v \operatorname{Im} G(x = 0, x' = 0, E - 2m_t + i\Gamma) \quad (29)$$

and

$$\rho_v = \left|Q_tQ_e + \frac{v_tv_es}{s - m_Z^2 + im_Z\Gamma_Z}\right|^2 + \left|\frac{v_ta_es}{s - m_Z^2 + im_Z\Gamma_Z}\right|^2 . \quad (30)$$

For $\Gamma_Z \to 0$ this equation is equivalent to the usual formula for e^+e^- production of nonrelativistic bound states. The nonvanishing width $\Gamma_t \gg \Lambda_{\text{QCD}}$ implies that Green's function is determined by short distances where QCD perturbation theory is valid. This is clear from a conceptual point of view and can also be proven by an explicit calculation of $\operatorname{Im} G$ [24, 27, 28]. This calculation sums all ladder diagrams (like that in Fig. 12) to a perturbative QCD potential and, as a result, gives us $\sigma(e^+e^- \to t\bar{t})$ as a function of s in the threshold region. It can be smoothly joined to the result of fixed (first) order perturbation theory and yields Figs 13(a),(b),(c) and 14.

Let us note that a potential can be calculated for Higgs exchange diagrams, too. However, for values of the Higgs mass, $m_H \geq 0(m_t)$, it is smaller than 3% of the gluon potential.

It is well known that from angular distributions of particles in scattering processes one can learn a lot about their properties (couplings). Therefore

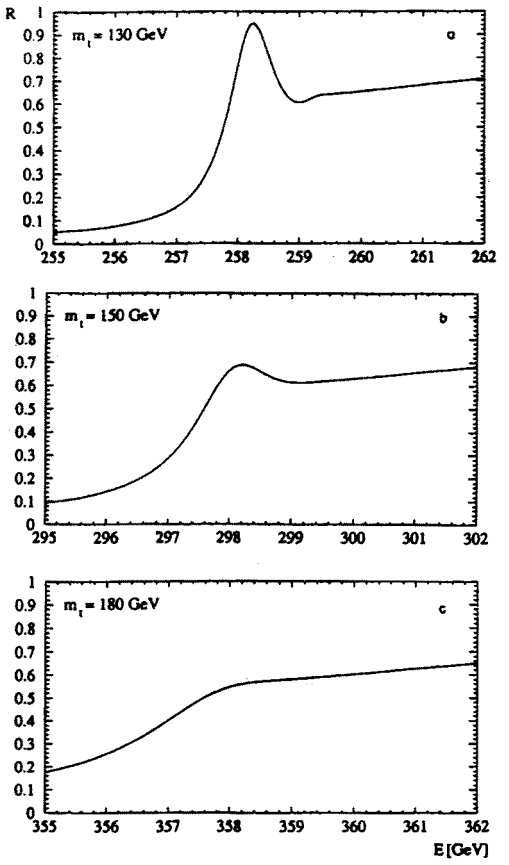

Fig. 13.

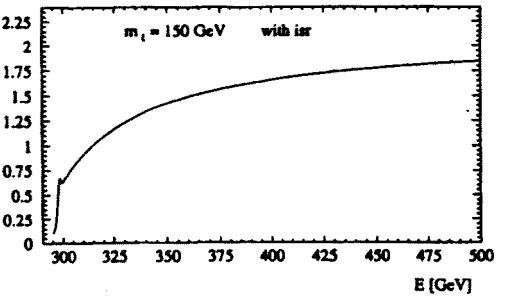

Fig. 14.

here we shall take some time to discuss the normalized angular distribution $(1/\sigma)(d\sigma/d\cos\theta)$. We have already given in (23) a general expression for it and in Eqs (25) and (26) the threelevel Standard Model results for

σ_U, σ_L and σ_P. In Fig. 15 we show the quantity $d\sigma/\sigma d\cos\theta$ graphically for $m_t = 150\text{GeV}$ and for several energy values $\sqrt{s} = 2m_t + \left\{ \begin{array}{c} 0.1 \\ 10 \\ 100 \end{array} \right\}\text{GeV}$. We see that the distribution is flat at threshold and receives a negative slope above threshold. The corresponding forward backward asymmetry is given in Fig. 16 as a function of beam energy. These curves are characteristic for the couplings of the top quark to the vector bosons as predicted by the Standard Model. Admixtures of other couplings will change the results of Figs 15 and 16 significantly. This has been examined in detail in [29] where, in the framework of an effective Lagrangian approach, new dimension six interactions of the top quark have been added to the Standard Model Lagrangian.

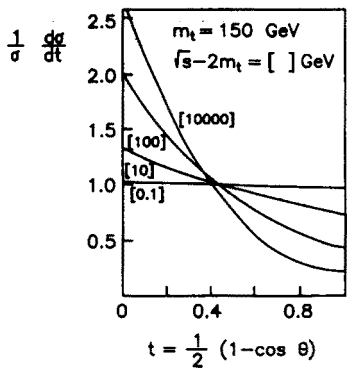

Fig. 15.

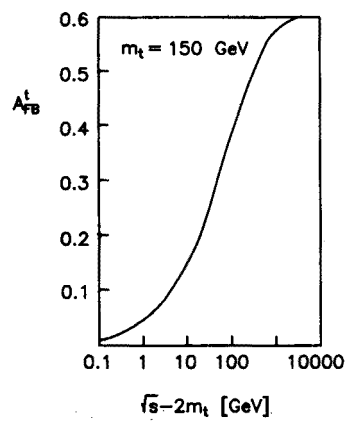

Fig. 16.

It is a question of some interest to see how far the expressions (25), (26) are distributed by higher order corrections. Since we know about the importance of the Coulomb singularity near threshold the question immediately arises how much the flat angular distribution which one encounters at threshold is affected. It turns out that the normalized angular distribution is not changed simply because the ladder diagrams (Fig. 12) responsible for the Coulomb singularity all give the same angular structure than the Born term. The Coulomb terms give rise to the same vector and axial vector vertex structure as the Born term. They do not contribute to the $\sigma_{\mu\nu}$ vertex term which usually arises in higher order calculations.

The upshot of these considerations is that at threshold the higher order corrections drop out for the ratio $d\sigma/\sigma$. One can verify with the help of (28) that this holds true to some extent even for energies well above thresholds. For example, a top quark with mass $m_t = 150\text{GeV}$ has at $\sqrt{s} = 500\text{GeV}$ an angular distribution $d\sigma/d\cos\theta$ with QCD corrections which vary between 13.1% (at $\cos\theta = 1$) and 9.1% (at $\cos\theta = -1$). Only at very high energies, $\sqrt{s} > 1\text{TeV}$, the angular dependence of the QCD corrections become really significant, approaching that of massless QCD
$\sigma_U = (1 + {}^1\!/_3\,\alpha_s/\pi)(\sigma_{VV} + \sigma_{AA})$, $\sigma_L = {}^2\!/_3\,(\alpha_s/\pi)(\sigma_{VV} + \sigma_{AA})$, $\sigma_P = \sigma_{VA}$. In any case, the full $m_t/\sqrt{s}$ dependence of the angular distribution including QCD corrections is given by (28). Note that nothing is known about electroweak corrections to the angular distribution.

The situation turns out to be even simpler if we look at angular distributions of decay products of the top quark *e.g.* the angle θ_μ between the muon of the decay $t \to b\mu^+\nu_\mu$ and the incoming e^- beam. This is a channel of particular interest because it gives a clear experimental signal. We shall see that QCD corrections are almost washed out to become independent of θ_μ so that the ratio $(1/\sigma)(d\sigma/d\cos\theta_\mu)$ is insensitive to higher orders and a clean device to study the couplings of the top quark. Let us now derive the θ_μ distribution in some detail.

When we were talking about top quark decay in Section 3 we had an unpolarized t quark in mind. However, the top quarks are produced in e^+e^- annihilation with a high degree of polarization that affects the distribution of jets and leptons after the decay. The polarization shows a strong forward backward asymmetry which in general alters the distribution as obtained from unpolarized quarks. The rest of this section is devoted to the study of this effect.

Let us consider the leading order process $e^+e^- \underset{\gamma,Z}{\longrightarrow} t\bar{t}$ with amplitude

$$M(e^+e^- \to t\bar{t}) = \frac{e^2}{s}\Big\{\bar{u}(t)Q_t\gamma_\mu v(\bar{t})\bar{v}(e^+)Q_e\gamma^\mu u(e^-) + \frac{s}{s - {m_Z}^2 + i\Gamma_Z m_Z}\bar{u}(t)(v_t + a_t\gamma_5)\gamma_\mu \times v(\bar{t})\bar{v}(e^+)(v_e + a_e\gamma_5)\gamma^\mu u(e^-)\Big\},$$

$$v_f = \frac{I_3^f - 2Q_f s_W^2}{2s_W c_W}, \quad a_f = \frac{I_3^f}{2s_W c_W}. \tag{31}$$

When squaring the amplitude one should make use of the standard relations

$$\sum v(\bar{t})\bar{v}(\bar{t}) = \frac{\bar{\not{t}} - m_t}{2m_t}\frac{1}{2}(1 + \gamma_5\bar{\not{s}}), \ldots \tag{32}$$

If one does not sum over polarization s and $\bar{s}$ of t and $\bar{t}$ the resulting cross section can be written in the form [30]

$$d\sigma = A(1 + a_\mu s^\mu + \bar{a}_\mu \bar{s}^\mu + c_{\mu\nu}s^\mu\bar{s}^\nu)dPS(e^+ + e^-; t, \bar{t}). \tag{33}$$

The coefficients A, a, $\bar{a}$ and c are functions of the couplings and of the fermion momenta. Similarly the semileptonic top decay rate which can be deduced from the matrix element

$$M(t \to b\mu^+\nu_\mu) = \frac{\frac{G_F}{\sqrt{2}}{m_W}^2}{{m_W}^2 - W^2 - i\Gamma_W m_W} \times \bar{u}(b)(1 + g_A\gamma_5)u(t) \times \bar{u}(\nu_\mu)\gamma_\mu(1 - \gamma_5)v(\mu^+), \quad g_A = -1, \tag{34}$$

has the form

$$d\Gamma = B(1 + b_\mu s^\mu)dPS(t; b, \nu_\mu, \mu^+), \tag{35}$$

where explicitly we have

$$B(1 + b_\mu s^\mu) = \frac{8G_F^2}{m_t}\frac{{m_W}^4}{({m_W}^2 - W)^2 + \Gamma_W^2 {m_W}^2}\Big\{(1 + g_A)^2[(t + m_t s)\nu_\mu][\mu^+ b] + (1 - g_A)^2[(t - m_t s)\mu^+][\nu_\mu b]\Big\}. \tag{36}$$

The anti top decay rate is given by the substitutions $t \to \bar{t}$, $b \to \bar{b}$, $\mu^+ \to \mu^-$, $\nu_\mu \to \bar{\nu}_\mu$, $s \to -\bar{s}$ and is of the form

$$d\bar{\Gamma} = \bar{B}(1 + \bar{b}_\mu\bar{s}^\mu)dPS(\bar{t}; \bar{b}, \bar{\nu}_\mu, \mu^-). \tag{37}$$

For the combined production and decay process one has to take the product $d\sigma d\Gamma d\bar{\Gamma}$ and has to sum over spinpolarizations using

$$\sum_{\sigma} 1 = 1\,,$$
$$\sum_{\sigma} s_\mu = 0\,,$$
$$\sum_{\sigma} s_\mu s_\nu = -g_{\mu\nu} + \frac{t_\mu t_\nu}{{m_t}^2}\,, \tag{38}$$

and similar for $\bar{s}$. This is very easily accomplished and yields

$$\begin{aligned} d\sigma(e^+e^- \to t\bar{t} \to b\bar{b}\mu^+\mu^-\nu_\mu\bar{\nu}_\mu) = \\ \Big[1 + a^\mu b^\nu\Big(-g_{\mu\nu} + \frac{t_\mu t_\nu}{{m_t}^2}\Big) + \bar{a}^\mu\bar{b}^\nu\Big(-g_{\mu\nu} + \frac{\bar{t}_\mu\bar{t}_\nu}{{m_t}^2}\Big) \\ + c^{\mu\nu}b^\alpha\bar{b}^\beta\Big(-g_{\mu\alpha} + \frac{t_\mu t_\alpha}{{m_t}^2}\Big)\Big(-g_{\nu\beta} + \frac{\bar{t}_\nu\bar{t}_\beta}{{m_t}^2}\Big)\Big] \\ \times AB\overline{B}\,dPS_2(e^+e^-;t,\bar{t})dPS_3(t;b,\mu^+,\nu_\mu)dPS_3(\bar{t};\bar{b},\mu^-,\bar{\nu}_\mu). \end{aligned} \tag{39}$$

If one likes, one can cast this in the form of a "theorem" as discussed in Ref. [31], for example. One has the usual term $AB\overline{B}$ plus 3 spin correlation terms which in Ref. [31] are written with the help of insertions $\ldots\gamma_5\gamma_\mu\ldots\big(-g_{\mu\nu} + (t_\mu t_\nu/{m_t}^2)\big)\ldots\gamma_5\gamma_\nu$ arising from the term $\sim \gamma_5 \not{s}$ and the spin summation rules (38).

Finite width effects for the Born term can be taken into account by introducing the propagators and off shell momenta for the top quarks in the matrix elements. They prove to be $< 1\%$ effects of the order of Γ_t/m_t.

In the following we want to describe the numerical effects of the spin correlation terms on the cross section. There are 3 important features of these terms which should be mentioned beforehand.

- First, they average out in the totally integrated cross section as well as sorts of energy distributions like the distribution in the muon energy $E(\mu^+)$. They are, however, important for angular distributions like $\theta_\mu := \not\sphericalangle\,(e^-,\mu^+)$ or $\theta_{+-} := \not\sphericalangle\,(\mu^+,\mu^-)$ (for the decay $e^+e^- \to t\bar{t} \to b\mu^+\nu_\mu\bar{b}\mu^-\bar{\nu}_\mu$) *etc.*
- Secondly, all spin correlation terms are of order $m_t/\sqrt{s}$ with respect to the spinaveraged term $AB\overline{B}$ and vanish in the high energy limit $(s \to \infty)$.
- Thirdly, all spin correlations which contribute to our angular distributions are proportional to a_e or a_t, *i.e.* they vanish in the limit of pure vector couplings. Furthermore, they are all of the form $VVVA$ or $VAAA$. Conversely, such $VVVA$ and $VAAA$ terms are not present

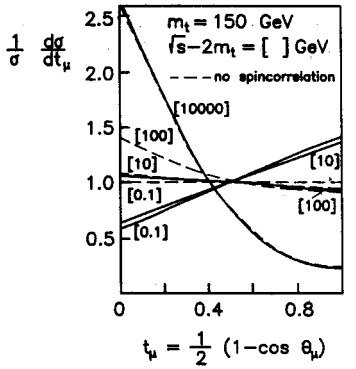

Fig. 17.a.

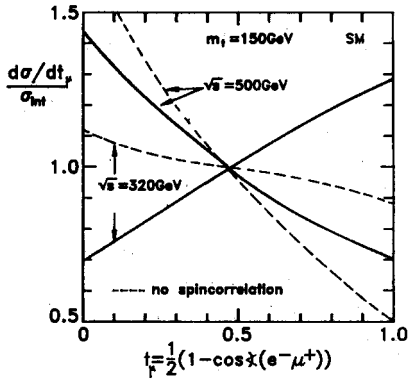

Fig. 17.b.

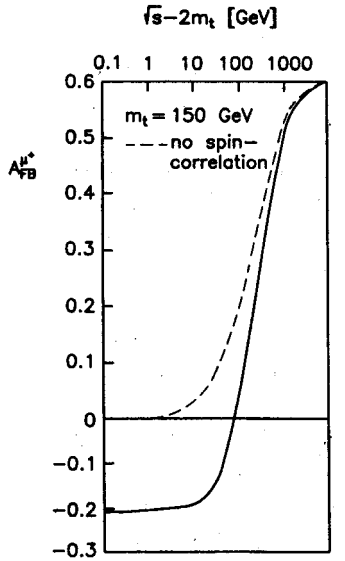

Fig. 17.c.

in the spinaveraged case ($s = \bar{s} = 0$), *i.e.* they consist solely of spin correlation terms.

In Fig. 17 the normalized distributions $(1/\sigma)(d\sigma/d\cos\theta_\mu)$ are shown for $m_t = 150\text{GeV}$ and several values of $\sqrt{s}$. We see that at threshold the distribution is uniform in θ_μ as long as spin terms are not taken into account. If this is done, however, even at threshold a relatively large (negative) forward backward asymmetry of the muons is induced.

In my opinion the θ_μ distribution is a very important observable because it inherits information about spin correlations and all Standard Model couplings of the Z and W to the top quark. Any change in these couplings leads to a significant deviation from the curves in Fig. 17. This has been established in Ref. [29] in the framework of an effective Lagrangian approach where dimension six interactions added to the Standard Model Lagrangian have been examined. In Fig. 18 it is established for the case of a $V + A$ interaction. By that we mean that the sign of a_t and of g_A in Eq. (31) and Eq. (34) is reversed.

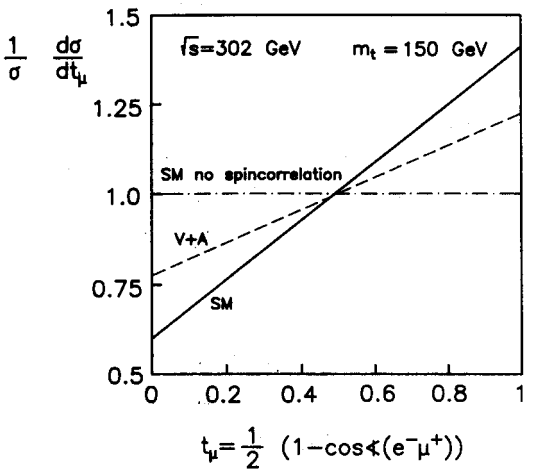

Fig. 18.

Finally, in Figs 19 we show the distribution of the cross section in $E(\mu^+)$ and in $\theta_{+-} := \measuredangle(\mu^+, \mu^-)$. These observables are not of so much interest as the θ_μ distribution because they depend more on the kinematical situation than on the underlying theory. For example, the steepening of the θ_{+-} distribution with increasing energy is a consequence of the back to back production of the top quarks and consequently of the muons at high energies.

What about radiative corrections? We have seen that QCD corrections can be rather large for the total cross section in particular near threshold

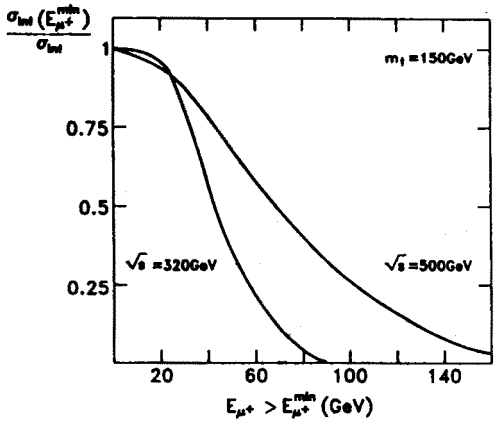

Fig. 19.a.

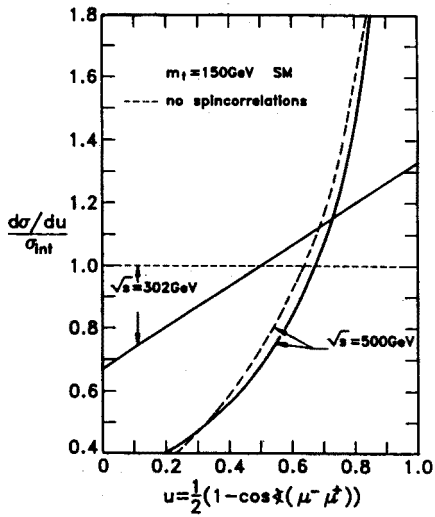

Fig. 19.b.

whereas the form of angular distributions of the top quarks are only affected far above threshold. Since heavy quark spins are not flipped by emission of low energy gluons, we expect QCD corrections to the polarization terms also to be universal. More precisely, the fact that only ladder diagrams (Fig. 12) contribute, is still true if one includes spinterms. Even more, these ladder contributions are still proportional to the Born term, a sufficient condition to guarantee angular independence of QCD corrections near threshold.

One can show by an explicit calculation that this remains true above threshold to a very good approximation, in fact to a better approximation than it was true for the distribution in $\theta = \sphericalangle(e^-, t)$. For example, a top quark with mass $m_t = 150\text{GeV}$ had at $\sqrt{s} = 500\text{GeV}$ an angular distribution

$(d\sigma/d\cos\vartheta)$ with QCD correction which vary between 13.1% (at $\cos\theta = 1$) and 9.1% (at $\cos\theta = -1$). If the top quark decays into a muon the QCD correction to $(d\sigma/d\cos\theta_\mu)$ varies between 11.2% (at $\cos\theta = 1$) and 9.5% (at $\cos\theta_\mu = -1$). We see that the effect of hard gluons is somewhat washed out in the θ_μ distribution.

Now the QCD corrections to the combined production and decay process $e^+e^- \to \mu^+ X$ are a sum of QCD corrections to the production vertex and to the decay vertex, and the numbers above account only for corrections at the production vertex. My conjecture is that gluon corrections to $(1/\sigma)(d\sigma/d\cos\theta_\mu)$ from the decay vertex are small, too. But this is something which still has to be proven.

REFERENCES

[1] F. Abe *et al.*, CDF Collaboration, *Phys. Rev. Lett.* **68**, 447 (1992).

[2] For a review see D. Schaile, P.M. Zerwas, DESY Report 91-106.

[3] H. Albrecht *et al.*, ARGUS Collaboration, *Phys. Lett.* **B192**, 245 (1987); M. Artuso *et al.*, CLEO Collaboration, *Phys. Rev. Lett.* **62**, 2233 (1989).

[4] J.V. Allaby *et al.*, CHARM Collaboration, *Z. Phys.* **C36**, 611 (1987); A. Blondel *et al.*, CDHF Collaboration, *Z. Phys.* **C45**, 361 (1990).

[5] See, for example, G. Burgers *et al.* in Z Physics at LEP1, Vol.1, p.55, CERN report 89-08 (1989).

[6] For a review, see G. Altarelli, Talk at the XIV Symposium on Lepton and Photon Interactions, Stanford, August 1989.

[7] See also G. Altarelli, Talk given at the 4th International Symposium on Heavy Flavour Physics Orsay, France, June 1991.

[8] The LEP Collaborations: ALEPH, DELPHI, L3, OPAL, CERN-PPE/91-232.

[9] W. Hollik *et al.*, Z Physics at LEP1, Vol.1, p.7, CERN report 89-08, (1989).

[10] G. Altarelli, R. Barbieri, *Phys. Lett.* **B253**, 161 (1990).

[11] M.E. Peskin, T. Takechi, *Phys. Rev. Lett.* **65**, 964 (1990).

[12] A. Sirlin, CERN preprint TH.5506/89 (1989).

[13] W. Beenakker, W. Hollik, *Z. Phys.* **C40**, 141 (1988).

[14] W. Celmaster, R.J. Gonsalves, *Phys. Rev.* **D21**, 3112 (1980).

[15] J. Jersak, E. Laermann, P.M. Zerwas, *Phys. Rev.* **D25**, 1218 (1982); G. Altarelli, B. Lampe, CERN-TH. 6424/92 (1992).

[16] B. Lampe, R. Mertig, in preparation; The possibility of a new $V+A$ interaction has been examined by R.D. Peccei *et al.*, *Nucl. Phys.* **B349**, 305 (1991).

[17] A. Denner, T. Sack, *Nucl. Phys.* **B358**, 46 (1991).

[18] M. Jeżabek, J.H. Kühn, *Nucl. Phys.* **B320**, 20 (1989).

[19] This is in close analogy to the discussion presented by G. Altarelli *et al.*, *Nucl. Phys.* **B208**, 365 (1982) for b decay.

[20] A. Czarnecki, M. Jeżabek, J.H. Kühn, *Nucl. Phys.* **B351**, 70 (1991).

[21] S. Dawson *et al.*, *Nucl. Phys.* **B303**, 607 (1988); W. Beenakker *et al.*, *Phys. Rev.* **D40**, 54 (1989).

[22] M. Diemoz *et al.*, *Z. Phys.* **C39**, 21 (1988); P.N. Harriman *et al.*, *Phys. Rev.* **D37**, 1161 (1988); *Phys. Rev.* **D42**, 798 (1990); G.J. Morfin, W.K. Tung, *Z. Phys.* **C52**, 13 (1991).
[23] See, for example, J.H. Kühn *et al.*, Top Quark (Theoretical Aspects), P. Igo-Kemenes *et al.*, Top Quark Physics (Experimental Aspects), Proc. of the 1991 Workshop on Future e^+e^- Colliders, Saariselkä, Finnland, September 1991.
[24] See, for example, J.M. Strassler, M.E. Peskin, *Phys. Rev.* **D43**, 1500 (1991).
[25] R.J. Guth, J.H. Kühn, *Nucl. Phys.* **B368**, 38 (1992); W. Beenakker *et al.*, *Nucl. Phys.* **B365**, 24 (1991); *Phys. Lett.* **B269**, 425 (1991).
[26] M.D. Tran, *Phys. Rev.* **D23**, 2769 (1981).
[27] V.S. Fadin, V.A. Khoze, *Sov. J. Nucl. Phys.* **48**, 309 (1988).
[28] M. Jeżabek, J.H. Kühn, T. Teubner, Karlsruhe preprint TTP 92-16 (1992).
[29] B. Lampe, INLO-PUB-6/92 Leiden 1992 preprint, to appear in *Phys. Lett.* **B**.
[30] S. Jadach, J.H. Kühn, MPI-PAE/PTh 64/86 (1986).
[31] S. Kawasaki *et al.*, *Prog. Theor. Phys.* **49**, 1656 (1973).